24th COBEM - 2017

24th ABCM International Congress of Mechanical Engineering
December 3-8, 2017, Curitiba, PR, Brazil

EXPERIMENTAL SETUP FOR A BENCH SCALE MULTIPLE DISKS TURBINE (TESLA TURBINE)

Conrado Ermel[1]
Paulo Smith Schneider[1]
André Thomazoni[1]
Charles Rech[2]
Júlio Vieira[1]
Gabriel Novo[1]

1-Federal University of Rio Grande do Sul, Porto Alegre, Brazil
conradoermel@gmail.com; pss@mecanica.ufrgs.br; andre@prosumir.com.br; julio@prosumir.com.br; gabrielgn_@hotmail.com
2-UniLasalle, Porto Alegre, Brazil
charlesrech@uol.com.br

Abstract. *This paper presents the assembling and commissioning of an experimental setup designed for the assessment of Multiple Disc Turbines (MDT). The workbench was built to essay MDT up to 1 kW mechanical output under controlled laboratory conditions. Compressed air is the driving working fluid, limited to the range of 2.0 to 4.5 bara, and some relevant output are reported, as working fluid mass flow rate, pressure and temperature. Steady state regime is established for several angular speed levels by means of a Foucault dynamometer, allowing for torque measurement. Sensors and workbench uncertainties are presented. Paper brings an experimental analysis of the isentropic efficiency of one MDT and compares it to literature. The achieved efficiency ranges from 9.7% to 12.0%, with ± 0.23% uncertainty, at 4.5 bara. Air mass flowrate is blocked at the turbine nozzle (Ma=1). Results are in accordance with the ones reported in literature, allowing to use the them for further analysis in numerical and analytical models.*

Keywords: *Tesla turbine, Multiple Disc Turbine, Low Availability Stream, Energy Recovery.*

Nomenclature

A_t – Nozzle cross-section area in the throat [m²]
c – Sound speed [m/s]
F – Force
f – Parameter (generic)
G – Mass flux [kg/m²-s]
h – Enthalpy
k – Isentropic coefficient
L – Length
$\dot{m}$ – Mass flow [kg/s]
$\dot{m}_t$ – Ideal mass flow rate [kg/s]
Ma – Mach number
P – Manometric pressure [barg]
R – Gas constant [J/Kg.K]
T – Temperature [K or °C]
$\dot{W}$ – Power [W]

Greek alphabet

ε – Flow pressure ratio
η_s – Isentropic Efficiency
u_c – Generic Parameter
ρ – Density [kg/m³]
τ – Torque [N.m]
ω – Angular speed [rad/s] or revolutions [RPM]

Subscripts

d – Discharge
i – Inlet
o – Outlet
s – Isentropic

1. INTRODUCTION

Multiple Discs Turbines MDT are mainly composed by a convergent nozzle, a set of parallel discs coupled to a shaft, called the rotor, placed in a casing, and exhaust channels for the working fluid. The nozzle accelerates the working fluid while MDT rotor converts the fluid momentum into mechanical energy in the shaft. The main difference to conventional turbines relays MDT rotor design, made with parallel discs equally separated, and attached to a common shaft. The

working fluid flows through the disc gaps, describing a spiral trajectory, as showed in Fig. 1(a). The first report of that constructive concept was done by Nikola Tesla in 1913, Fig. 1(b), which patented his prototype under code 1061206 (Tesla, 1913). For this reason, MDT are also known as Tesla Turbine.

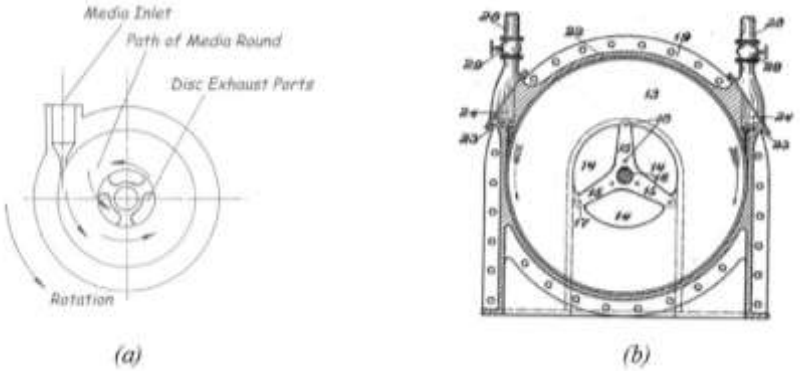

Figure 1. Tesla Turbine: a) Fluid trajectory, b) Tesla's patent (Cairns, 2003)

After his patent, and based upon data from an experimental unit, Tesla built a 100 HP steam driven turbine. Larger units were built, including a 200HP, 18" rotor (Cairns, 2013). Although its promising application due to construction simplicity, the MDT's research stayed in hold for a relatively long time. Some aspects that contributed to this situation were the low quality of materials from that time and low available torque (Cairns, 2013). Some latter studies were carried out by Leaman (1950) and Gruber (1960). Rice compiled some of these works and performed an analytical and experimental investigation with several MDTs, indicating its possible application in low grade energy streams (Rice, 1965).

Several authors studied the design, application and efficiency of MDTs. However, there is a divergence concerning the isentropic efficiency between the results found by the numerical simulation and analytical works (Couto, *et al*., 2006, Guha and Sengupta, 2013 and Romanin and Carey, 2011) and the experimental studies (Cairns, 2003, Batista, 2009, Lemma *et al*., 2008 and Maidana, 2015). Although the theoretical studies present more optimistic results, the experimental works generally find much lower efficiency values. Despite the challenges presented by the MDT, this type of device has been researched and applied in different sectors of industry. In automotive industry, Hasan (2016) investigated the viability of Tesla turbine as drivers for air-conditioning compressors. Results indicated that MDTs are a low cost solution for energy recovery. Recently, Song and Li (2017) developed a one-dimensional model to predict the efficiency of Tesla turbines applied to ORC (Organic Rankine Cycle). Results indicated that Tesla turbine has potential in ORC applications.

Paper review points out that MDT can be a viable device for energy recovery applications, mainly linked to low availability streams. State of the art also reveals that there is an opportunity to increase MDT efficiency, and the present work is focused on the assembling of an experimental workbench for small scale prototypes, aiming to reach stable test conditions that will allow for reliable research on design improvement of small scale multi disk turbines.

2. TURBINE MODELING SPECIFICATION

The turbine designed in this work is a small-scale prototype for low energy streams. In Fig.2. casing was made of machined steel, nozzle from stainless steel, rotor discs from aluminum with proper surface finishing. Previous studies (Cairns, 2003) helped to define some dimensions, as disc gap proposed by Rice (1965). The rotor prototype was built with four parallel 300mm diameter discs, with 1mm of disc gap. The bearings were selected to allow high angular speed values and to fix axially the MDT, so the rotor gap will be always aligned with the nozzle.

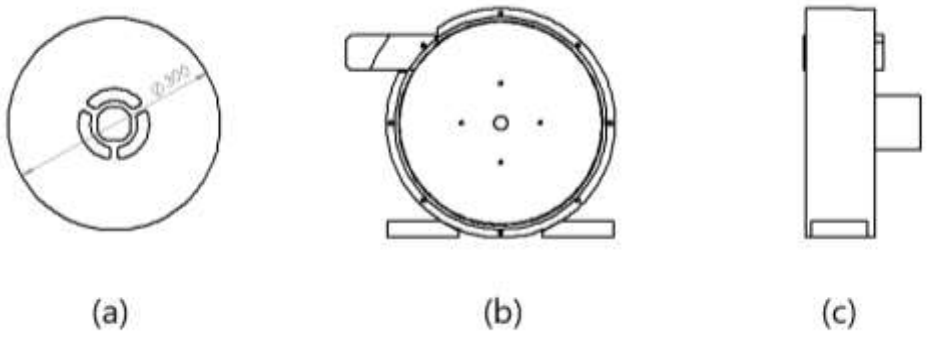

Figure 2. Multiple disk turbine a) Individual disc dimension, b) Casing front-view, c) Casing side-view

Nozzle plays an important role in MDT operation and efficiency (Rice, 2003). MDT prototype is equipped with a single rectangular nozzle, convergent shaped with a cross-section area of 30,54 mm² (4,1mm x 7,45mm). The prototype overall view is displayed in Fig. 3.

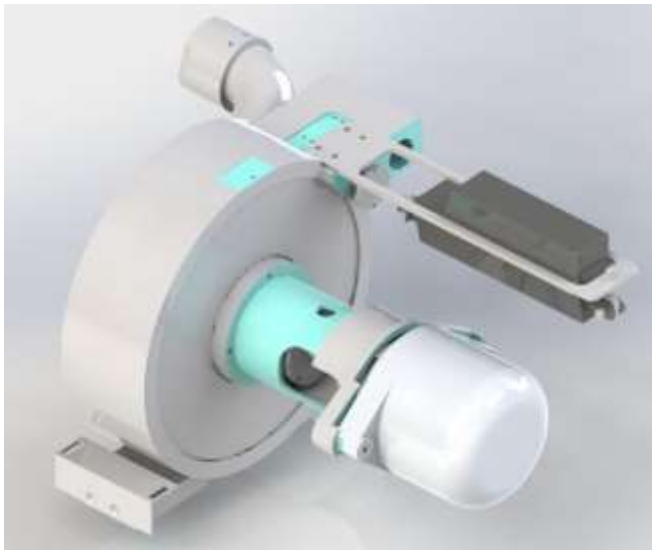

Figure 3. Isometric view of the MDT prototype

According to Dixon, 1998, expansion process through an adiabatic turbine can be expressed as presented in the Mollier diagram in Figure 4.

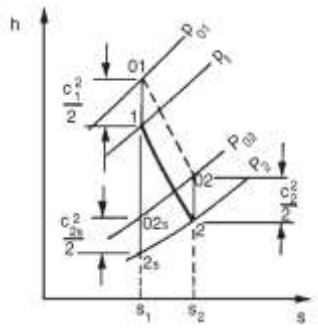

Figure 4. Mollier diagram for the expansion of the working fluid expansion on a turbine (Dixon, 1998)

Turbine maximum theoretical work is given by the isentropic expansion process from line 01-02s, as referred in the diagram. Small differences of inlet and outlet kinetic energy allow for neglecting its contribution and consider the expansion processes from point 1 to point 2, whereas the ideal isentropic expansion is referred by line 1-2s. Turbine isentropic efficiency can be expressed as:

$$\eta_s = \frac{\tau\omega}{\dot{m}_t(h_1 - h_{2s})} \tag{1}$$

where τ is the measured shaft torque, ω is the measured angular speed, $\dot{m}_t$ the ideal mass flow rate at the nozzle throat, h_1 and h_{2s} are the working fluid specific enthalpies at the turbine inlet and isentropic outlet.

The specific enthalpy h_{2s} depends on the working fluid outlet pressure P_2, which can be calculated by the pressure ratio for an ideal gas isentropic expansion, reported by Sonntag et al. (2009).

$$\frac{P_1}{P_2} = \left[1 + \frac{k-1}{2} Ma^2\right]^{\frac{k}{k-1}} \tag{2}$$

where P_1 is the inlet pressure, k is the isentropic coefficient based on inlet data, and Ma the flow Mach number. Inlet to outlet pressure relation is also expressed by the flow pressure ratio ε, presented in Eq. (3).

$$\varepsilon = \frac{P_2}{P_1} \tag{3}$$

That last ratio indicates whether the flow is sonic, supersonic, or subsonic flow, as follows:

- $\varepsilon > \varepsilon^*$ then the flow is subsonic;
- $\varepsilon = \varepsilon^*$ then the flow is sonic - Considering air with k = 1.4, ε^*= 0.528;
- $\varepsilon < \varepsilon^*$ then the flow is supersonic;

Flow through convergent nozzles is limited to subsonic and sonic flow conditions and its maximum flow rate $\dot{m}_t$ is calculated by Eq. (4), considering an isentropic expansion with Ma = 1.

$$\frac{\dot{m}_t}{A_t} = \frac{P_1}{\sqrt{T_1}}\sqrt{\frac{k}{R}}\left[\frac{1}{\left[\frac{k+1}{2}\right]^{\frac{k+1}{2(k-1)}}}\right] \tag{4}$$

where A_t is the nozzle cross-section area at the throat, R is the specific gas constant, k is the isentropic coefficient and T_1 is the fluid temperature at the nozzle inlet.

3. WORKBENCH CHARACTERISTICS

A workbench was built to test the MDT prototype, shown in Fig 5.

(a) (b)

Figure 5. Workbench: a) Front view, b) Back view

Filtered air was adopted as the working fluid, fed by a dedicated compressor, and ranged by a control valve. The workbench average ambient pressure was taken as 1.01325 bara.

3.1 Workbench General Specification

Figure 6 gives an overview of the workbench, its components and instruments.

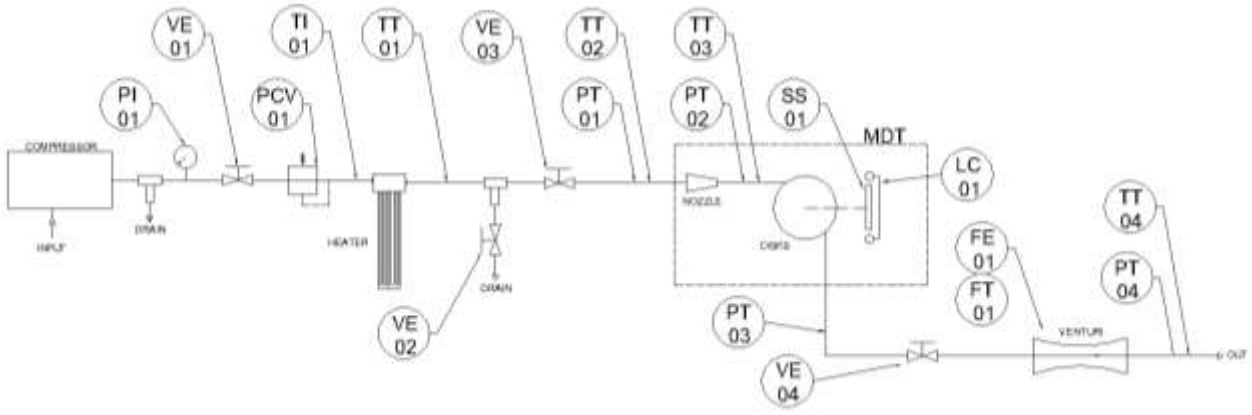

Figure 6. Workbench basic scheme

The dashed line around the MDT area represents the turbine, composed by its nozzle, housing and rotor. Tags indicate instruments and sensors along the flow line, as manometers, thermometers, volumetric-flow meters, etc. Turbine power

is measured by torque and angular speed measurements under variable load, imposed by a Foucault dynamometer, assembled to the shaft (Fig. 7).

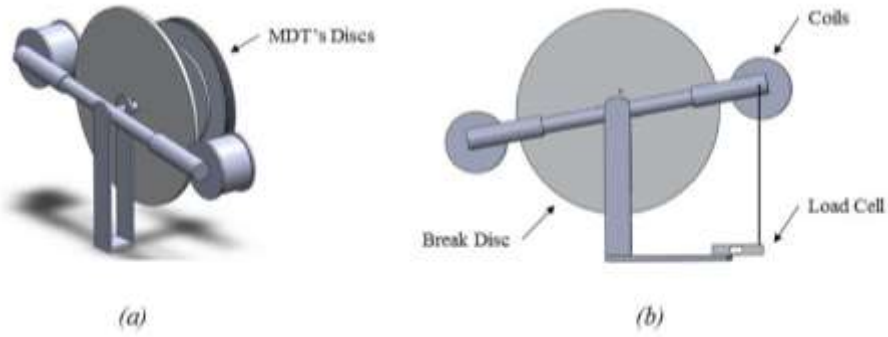

Figure 7. Foucault brake: (a) Isometric view, (b) Basic design

Disc breaking is controlled to obtain the desired torque on the rotor axis by the imposition of a variable magnetic field, generated by the side coils. Torque is measured by a load cell attached to the dynamometer arm.

Static pressure is monitored at the air discharge, and a Venturi device is used to measure airflow. This last one was manufactured according with NBR 5167-1:2008.

Acquisition system was assembled to capture and treat data, allowing to calculate dependent parameters such as torque, power, airflow and angular speed.

3.2 Instrumentation

Workbench main sensors and instruments are declared in Table 1, following the tag symbolism presented in Fig. 6, followed by their specific measuring range and uncertainty.

Table 1. Workbench list of sensors and instruments, according to Fig 6.

TAG	Description	Model	Range	Uncertainty
PI-01	Manometer (main line)	N/A	0-17 bar	Class B
VE-01	Sphere valve ½" – Inlet 1	-	-	-
VR-01	Pressure regulator	-		
TI-01	Thermometer	-	-	-
TT-01	Temp. sensor – Heater output	PT-100	-	-
VE-03	Sphere valve ½" – Inlet 2	-	-	-
TT-02	Temp. sensor – Nozzle inlet	Type K thermocouple	-200 a 1250 °C	± 0.5 °C
PT-01	Pressure sensor – Nozzle inlet	PS-10B	0-10 bar	± 0.05 bar (0,5% FS)
TT-03	Temp. sensor – Housing	Type K thermocouple	-200 a 1250 °C	± 0.5 °C
PT-02	Pressure sensor – Housing	PSE550-X501	0 to1 kPa	± 0.03 kPa (3% FS)
LC-01	Load cell – Torque Measurement	Bonad - Bnd- lc5.0	5 kgf	± 0.00005 (0,001% FS)
SS-01	Revolution sensor	BR200DDTN	-	-
PT-03	Pressure sensor – Turbine outlet	PSE550-X501	0 to1 kPa	± 0.03 kPa (3% FS)
VE-04	Needle valve	-	-	-
FE-01	Primary flow element – Venturi	-	-	-
FT-01	Differential pressure sensor	MPXV7002	-2 a 2 kPa	± 0.125 kPa (6.25% FS)
PT-04	Pressure sensor – System outlet	MPX4115	15 a 115 kPa	± 0.01725 kPa (1.5% FS)
TT-04	Temp. sensor – System outlet	Type K thermocouple	-200 a 1250 °C	± 0.5 °C
--	Caliper – (To measure nozzle area)	Mitutoyo	0 – 150mm	0.05mm

FS = full scale

The acquired variables allow to calculate torque τ and power $\dot{W}$, given by:

$$\tau = FL \quad (5)$$

$$\dot{W} = \tau\omega \quad (6)$$

where F is the load cell reading of the scalar component of force (LC-01), L is the lever arm and ω is the angular speed (SS-01). The Venturi device allows for the air mass-flow rate calculation, based on the reading of outlet air pressure and temperature (PT-04; TT-04), and the inlet to through nozzle differential pressure (FT-01).

3.3 Uncertainty

The combined uncertainty u_c of a given calculated parameter *f* was estimated by the Taylor and Kuyatt (1994) relation, given by Eq. (7).

$$u_c^2(f) = \sum_{i=1}^{N} \left(\frac{\partial f}{\partial x_i}\right)^2 u_i^2(x_i) + 2\sum_{i=1}^{N-1} \quad \sum_{j=i+1}^{N} \frac{\partial f}{\partial x_i}\frac{\partial f}{\partial x_j} u_i\left(x_i, xd_j\right) \qquad (7)$$

where u_i is the uncertainty of the *i* instrument, and its measured value, calculated with the aid of the Engineering Equation Solver (EES) software.

Turbine isentropic efficiency η_s, Eq. (1), is an important metric whenever turbine performance is to be compared. Efficiency combined uncertainty is calculated by Eq. (7), and depends on its input parameters, whose individual uncertainties are once more calculated by that same equation. Results for the input parameters and the turbine isentropic efficiency η_s are displayed in Table 2.

Table 2. Individual uncertainties related to the determination of turbine efficiency based on data from Table 1.

Variable	Relative Uncertainty
Measured mass flow rate ($\dot{m}$)	6.03%
Nozzle throat area (A_t)	1.23%
Torque (τ)	0.2064%
Power ($\dot{W}$)	0.2123%
Enthalpy (h)	0.2633%
Turbine isentropic efficiency η_s Eq. (1)	~ 2%

Preliminary results showed a combined uncertainty around 2%, mainly driven by the mass flow rate uncertainty.

4. RESULTS

Assessment of MDT performance is reported for a single inlet pressure and temperature. The Foucault dynamometer was used to impose several levels of brake reaction, allowing to measure process parameters, such as pressure, temperature, mass flow rate and torque for each angular speed.

Firstly, turbine was set to operate without any brake restriction, leaving rotor to achieve its stable running condition. Foucault dynamometer was then turned on and progressively imposed brake restrictions, and revolutions were stabilized for five different levels. More than 6,000 readings were recorded and the Chauvenet criteria was employed to eliminate spurious data.

The measuring routine presented in latest section yielded the database reported in next table.

Table 3. Experimental results for inlet air pressure of 4.5 bara for 6 replications with distinct angular speed.

Parameter	**TAG**	**EU**	**#1**	**#2**	**#3**	**#4**	**#5**	**#6**
Revolutions	SS-01	[RPM]	**7040**	**6536**	**6083**	**5517**	**5123**	**4018**
Torque[(1)]	LC-01	[Nm]	0.448	0.534	0.613	0.703	0.771	0.923
Power	[-]	[W]	330.7	365.6	390.5	406.5	414.0	388.3
Measured mass flow rate	FT-01	[kg/s]	0.031	0.032	0.032	0.031	0.032	0.032
Nozzle inlet Temp.	TT-02	[K]	295.4	296.4	296.5	297.2	297.8	297.7
Housing Temp.	TT-03	[K]	292.5	293.4	293.7	294.3	295.1	294.9
Discharge Temp.	TT-04	[K]	291.1	291.7	291.7	292.1	292.4	292.2
Nozzle Inlet Pressure	PT-01	[bara]	4.527	4.560	4.546	4.543	4.540	4.588
Housing Pressure	PT-02	[bara]	1.454	1.453	1.457	1.448	1.452	1.449
Rotor Outlet Pressure	PT-03	[bara]	1.018	1.018	1.018	1.018	1.018	1.018
Discharge Pressure	PT-04	[bara]	1.015	1.015	1.015	1.014	1.014	1.014

(1) measured at 25°C / EU: Engineering Units

Tests were performed from higher to lower angular speed and captured an inverse behavior of torque. Power followed a similar trend, but with a nonlinear tendency. Air mass flow rate presented small oscillations of the order of 0.001 kg/s, which is lower than its uncertainty (see Table 2) and therefore can be considered as constant. All temperatures and pressures presented insignificant variation (lower than its uncertainties – see Table 1).

MDT flow condition can be defined by comparing ε to its reference ε^*, and the ideal mass flowrate $\dot{m}_t$ to the measured mass flowrate (Table 3, FT-01). Results are displayed in Table 4.

Table 4. Flow condition in MDT for inlet air pressure of 4.5 bara for 6 replications with distinct angular speed

Parameter	TAG	EU	#1	#2	#3	#4	#5	#6
Revolutions	SS-01	[rpm]	**7040**	**6536**	**6083**	**5517**	**5123**	**4018**
Nozzle Inlet Pressure	PT-01	[bara]	4.527	4.560	4.546	4.543	4.540	4.588
Nozzle inlet Temp.	TT-02	[K]	295.4	296.4	296.5	297.2	297.8	297.7
Discharge Pressure	PT-04	[bara]	1.015	1.015	1.015	1.014	1.014	1.014
ε	[-]	[-]	0.22	0.22	0.22	0.22	0.22	0.22
$\dot{m}_t$	[-]	[kg/s]	0.032	0.032	0.032	0.032	0.032	0.032

Pressure Ratio ε was calculated with Eq. (3) using values of PT-01 and PT-04 as P_1 and P_2, respectively. Ideal mass flow rate $\dot{m}_t$ is calculated from Eq. (4) using PT-01 as P_1, TT-02 as T_1 and k was defined using EES Thermodynamic table for the inlet thermodynamic state.

Values for the ideal air mass flowrate $\dot{m}_t$ was compared to measured mass flow rate $\dot{m}$ (Table 3) and indicated that MDT achieved its maximum amount of mass flow rate across its control volume, since both mass flowrates can be taken as similar, meaning that a limit value was reached, known as the blocked condition. Such condition was proposed along the turbine design process, given by the pressure ratio $\varepsilon < \varepsilon^*$ (0.528 for k = 1.4).

Turbine efficiency assumes different values according to the measured operational conditions, as shown in the next equation, based on Eq. (1):

$$\eta_s = \frac{\tau[LC-01]\ \ \omega[SS-01]}{\dot{m}_t\ (Eq.4)\ (h_1[\mathrm{PT-01;TT-02}] - h_{2s}[\mathrm{PT-04}\ ; s_{2s}(\mathrm{PT-04}; s_1])} \qquad (8)$$

Eq. (4) was calculated for P_1 from PT-01 and T_1 from TT-02, and enthalpies are function of the air thermodynamic state at turbine inlet and outlet. Results for MDT efficiency are displayed in next table.

Table 5. MDT efficiency for inlet air pressure of 4.5 bara for 6 replications with distinct angular speed

Parameter	TAG	EU	#1	#2	#3	#4	#5	#6
Revolutions	SS-01	[RPM]	**7040**	**6536**	**6083**	**5517**	**5123**	**4018**
Nozzle Inlet Pressure	PT-01	[bara]	4.527	4.56	4.546	4.543	4.54	4.588
Nozzle inlet Temp.	TT-02	[K]	295.4	296.4	296.5	297.2	297.8	297.7
Discharge Pressure	PT-04	[bara]	1.015	1.015	1.015	1.014	1.014	1.014
s_1	[-]	[J/kg-K]	6.421	6.419	6.420	6.423	6.425	6.422
h_1	[-]	[J/kg]	295.574	295.565	295.670	296.379	296.987	296.872
h_{2s}	[-]	[J/kg]	192.450	192.043	192.281	192.724	193.156	192.499
Efficiency η_s [Eq. (8)]	[-]	%	9.86	10.78	11.57	12.03	12.26	11.31
Absolut Uncertainty			0.23	0.22	0.23	0.24	0.24	0.23

MDT efficiency displayed a slight nonlinear tendency. Its behavior is compared to the one reported by Rice (1965), and presented in Figure 8.

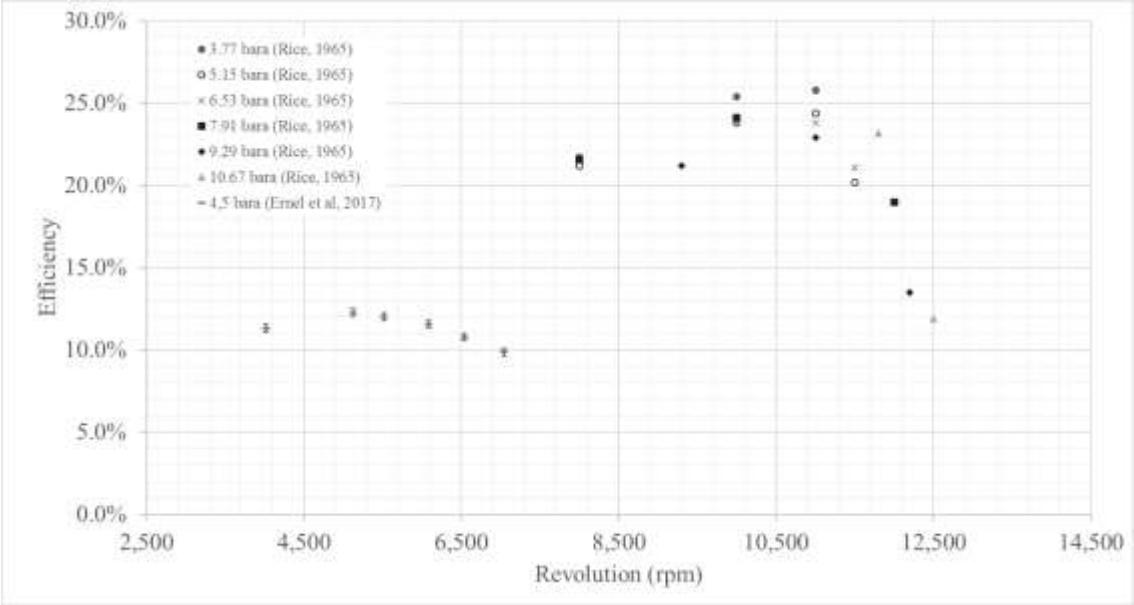

Figure 8. Measured MTD efficiencies as a function of revolution for different operational conditions, with data from Rice (1965), and the present work

Rice MDT (Rice, 1965) was built with a rotor diameter 60% bigger than the one of the present work, and recorded higher angular speed. Both efficiencies showed similar nonlinear tendency as a function of the angular speed, however Rice´s prototype reached better marks. In both cases, airflow reached $Ma = 1$ and underexpanded condition (values of ε in Table 5).

Rice MDT architecture is similar to the one tested on the present work, but was built with different number of nozzles and disks, and was operated at different inlet conditions, which can explain efficiency differences.

5. CONCLUSIONS

The main goal of this work was to build and operate a setup able to perform the experimental investigation of bench scale multiple disks turbines. Sensors were selected in order to measure specific key quantities that allow for the assessment of MDT prototypes, connected to a supervisory code. A MDT was also built as first approach to the project and tests were performed to measure inlet and outlet operational conditions of the working fluid, turbine torque and power. Efficiency was measured for a 4.5 bara airflow inlet pressure and displayed calculated values around 10%, with a nonlinear tendency, with absolute uncertainty of about ± 0.23%. Results were compared to the ones from Rice (1965), displaying similar trends, although the tested machines are quite different regarding dimensions, number of nozzles and were tested with higher levels of pressure.

The experimental setup will allow for further investigation on MDT development, concerning a detailed analysis on the causes of losses in MDT efficiency, since recent works like Guha (2013) suggested that it is possible to achieve higher efficiencies.

6. ACKNOWLEDGEMENTS

Ermel acknowledges the financial support from CNPq for his Msc grant; Smith Schneider acknowledges the research grant (CNPq-PQ 305357/2013-1).

7. REFERENCES

ABNT NBR, *ISO 5167-1:2008*, “Medição de vazão de fluídos por dispositivos de pressão diferencial, inserido em condutos forçados de seção transversal circular”, 2008, < http://www.abntcatalogo.com.br/norma.aspx?ID=001541>.

Batista, J. C., 2009, *Microgeração de Energia Elétrica (abaixo de 100 kW) Utilizando Turbina Tesla Modificada.* Ph.D. thesis, Universidade Estadual Paulista, Guaratinguetá, SP.

Cairns, W. M. J., 2003, *The Tesla Disc*, 1 vols. Barrow Farm, Rode, Frome, Somerset: Camden Miniature Steam Services, Great Britain, 2nd edition.

Couto, H., Duarte, J. B. and Bastos-Netto, D., 2006, "The Tesla Turbine Revisited," *Asia-Pac. Int. Symp. Combust. Energy Util.*, n°8, p.7.

Dixon, S.L, 1998, *Fluid Mechanics, Thermodynamics of Turbomachinery.*, Butterworth & Heinemann, Burlington, MA 4nd edition.

Gruber, E.L., 1960. An *Investigation of a Turbine with a Multiple-Disk Rotor*. MS. thesis, Arizona State University.

Guha, A. and Sengupta, S., 2013, "The fluid dynamics of the rotating flow in a Tesla disc turbine," *Eur. J. Mech. - BFluids*, vol. 37, p. 112–123.

Hasan, A. M., 2016, "Investigating the Possibility of Using a Tesla Turbine as a Drive Unit for an Automotive Air-Conditioning Compressor Using CFD Modeling," *ASHRAE*, n°OR-16-012, p. 13.

Leaman, A.B., 1950. *The Design, Construction and Investigation of a Tesla Turbine*. MS. thesis, University of Maryland.

Lemma, E., Deam, R. T., Toncich, D., and Collins, R., 2008, "Characterization of a small viscous flow turbine", *Experimental Thermal and Fluid Science*, vol. 33, n°33, p. 96–105, 2008.

Maidana, C. F., 2015, Desenvolvimento de Turbinas de Múltiplos Discos Estudo de Modelos Analíticos e Análise Experimental, Ph.D. thesis, Universidade Federal do Rio Grande do Sul, Porto Alegre.

Rice, W., 1965. "An analytical and experimental investigation of multiple-disk Turbines". *Journal of Engineering for Power*, p. 29-65.

Rice, W., 2003, *Handbook of Turbomachinery*, Marcel Dekker, INC, Tempe, Arizona 2nd edition, vol. 2.

Romanin, V. D. and Carey V. P., 2011, "*An integral perturbation model of flow and momentum transport in rotating microchannels with smooth or microstructured wall surfaces*", vol. 23, p. 12,

Song, J., Gu, C., and Li, X., 2017 "Performance estimation of Tesla turbine applied in small scale Organic Rankine Cycle (ORC) system", *Applied Thermal Engineering*, n°110, p. 318–326.

Taylor, B.N. and Kuyatt, C.E., 1994, Guidelines for Evaluating and Expressing the Uncertainty of NIST Measurement Results, *NIST – National Institute of Standard and Technology*, vol. 2.

Tesla N., "Turbine," 1 061 206, 06-May-1913.

8. RESPONSIBILITY NOTICE

The authors are the only responsible for the printed material included in this paper.